LASER INTERFEROMETER GRAVITATIONAL WAVE OBSERVATORY
- LIGO -
CALIFORNIA INSTITUTE OF TECHNOLOGY
MASSACHUSETTS INSTITUTE OF TECHNOLOGY

Technical Note	**LIGO-T960116-00 - D**	07/31/96

Modal Model Update 4

Mode Mismatch

Daniel Sigg

Distribution of this draft:

ASC

This is an internal working note
of the LIGO Project.

California Institute of Technology
LIGO Project - MS 51-33
Pasadena CA 91125
Phone (818) 395-2129
Fax (818) 304-9834
E-mail: info@ligo.caltech.edu

Massachusetts Institute of Technology
LIGO Project - MS 20B-145
Cambridge, MA 01239
Phone (617) 253-4824
Fax (617) 253-7014
E-mail: info@ligo.mit.edu

WWW: http://www.ligo.caltech.edu/

1 ABSTRACT

This technical note describes an implementation of the modal model which includes transverse modes up to second order. This code is used to investigate the influence of mode matching on the performance of LIGO. In section 2 the modal space representation of the mode mismatch operator is derived. In section 3 a wavefront sensing scheme for mode matching using a circular photodiode is developed. In section 4 the insertion of the mode mismatch operator into the interferometer equations is presented, whereas in section 5 the mode matching is parametrized as waist size and position mismatch. Section 6 calculates the sensitivity of the wavefront sensing to mode mismatch and Section 7 calculates the gravitational wave signal induced by a mode mismatch. Section 8 looks at the signal-to-noise loss due to errors in the radii of curvature of the test mass mirrors.

It is shown that wavefront sensors measuring the reflected light from the interferometer and using the non-resonant sideband pair are a good solution to mode match the input beam to the interferometer. To prevent a degradation of the gravitational wave sensitivity of more than 0.5%, it is required that the radius of curvature of the recycling mirror be matched to its nominal value given by the arm cavity parameters with a precision of ±100 m.

2 MODE MISMATCH OPERATOR

A mode mismatch can be seen as a mismatch in either curvature or spot size between the resonating eigenmode of a cavity and its input beam. In both cases the mismatch has a circular symmetry and can be described in first order as an excitation of a ‘donut’ mode. This ‘donut’ mode is a linear combination of the TEM_{20} and the TEM_{02} (Hermite-Gaussian) modes.

$$U_{\text{donut}} = \frac{1}{\sqrt{2}}(U_{20} + U_{02}) \tag{1}$$

In the modal space representation one can generally write a mode mismatch as a simple basis transformation between a basis defined by the input beam and a basis defined by the cavity eigenmodes. Hence, the mode mismatch operator K is a unitary operator:

$$K_{mn,\,kl} = \langle \overline{mn} | kl \rangle \tag{2}$$

where $|kl\rangle$ and $|\overline{mn}\rangle$ denote the old and the new basis vectors, respectively. As it turns out, the calculation of the mode mismatch operator K can be greatly simplified, if it is done at the z-position z_w, where the spot sizes of the two bases are equal. Such a position always exist, if the two basis sets share the same optical axis. And it is always possible do make the calculation at this position, since the propagation and the basis transformation commutates, i.e. it doesn’t matter, if a beam is first propagated from z to z_w and then changed into the new basis or if it is first transformed into the new basis and then propagated from z to z_w:

$$K_{mn,\,kl}\big|_z = \sum_{op,\,qr} \bar{P}^{\dagger}{}_{mn,\,op} K_{op,\,qr}\big|_{z_w} P_{qr,\,kl} \tag{3}$$

where $P_{qr,\,kl}$ and $\bar{P}_{mn,\,op}$ propagate the beam from z to z_w in the old and the new basis, respectively. Since the spot size $w(z_w)$ is equal for the two bases at position z_w, the new basis vectors can be written as the old ones times a factor given by the curvature mismatch only,

$$|\overline{mn}\rangle \;=\; \exp\left[-i\frac{k}{2}(x^2+y^2)\left(\frac{1}{R'}-\frac{1}{R}\right)\right]|mn\rangle \tag{4}$$

and the bra-ket product of eqn. (2) reduces to

$$\langle\overline{mn}|kl\rangle\big|_{z_w} \;=\; \langle mn|\exp\left[i\frac{k}{2}(x^2+y^2)\left(\frac{1}{R'}-\frac{1}{R}\right)\right]|kl\rangle \equiv \sum_{op,\,qr}\langle mn|\exp[im|op\rangle T^{MM}_{op,\,qr}\langle qr|]|kl\rangle \tag{5}$$

$$\text{with}\;\; T^{MM}_{op,\,qr} \;=\; \langle op|\left(\frac{\sqrt{2}x}{w(z_w)}\right)^2+\left(\frac{\sqrt{2}y}{w(z_w)}\right)^2|qr\rangle \;\;\text{and}\;\; m \;=\; \frac{kw(z_w)^2}{4}\left(\frac{1}{R'}-\frac{1}{R}\right) \tag{6}$$

where R and R' are the radii of curvature at position z_w for the old and the new basis vectors, respectively, and $T^{MM}_{op,\,qr}$ is the z-independent generator of the mode mismatch operator. Notice, that the right hand side of eqn. (5) only involves the old basis vectors.

Multiplying the operator (x^2+y^2) by $H_q(x)H_r(y)/H_q(x)H_r(y)$ and using the recursion relations for the Hermite polynomials (see appendix A of ref. [1]) the mode mismatch generator can be written as:

$$\begin{aligned} T^{MM}_{op,\,qr} \;=\; & \delta_{p,\,r}\left\{\frac{1}{2}\sqrt{o(o-1)}\,\delta_{o,\,q+2}+\left(q+\frac{1}{2}\right)\delta_{oq}+\frac{1}{2}\sqrt{q(q-1)}\,\delta_{o,\,q-1}\right\}+ \\ & \delta_{o,\,q}\left\{\frac{1}{2}\sqrt{p(p-1)}\,\delta_{p,\,r+2}+\left(r+\frac{1}{2}\right)\delta_{p,\,r}+\frac{1}{2}\sqrt{r(r-1)}\,\delta_{p,\,r-2}\right\} \end{aligned} \tag{7}$$

where $\delta_{m,\,n}$ denotes the Kronecker delta. Applying the mode mismatch operator on the fundamental mode excites in first order only a donut mode:

$$K(m)\big|_{z_w}U_{00} \;=\; (1+im)U_{00}+imU_{\text{donut}}+O(m^2) \tag{8}$$

As seen from the above equation, a curvature mismatch also changes the phase of the fundamental mode in first order. Sometimes, the mode mismatch operator K^{-} which describes a beam coming from the other direction is needed,

$$K^{-} \;=\; \langle mn|\bar{kl}\rangle \tag{9}$$

It is important to recognize that this operator is not the inverse of the operator K. Propagating backwards is changing the sign of the z-coordinate and the order in which the curvature mismatch is calculated, but it is also changing the sign of the radii of curvature, i.e.

$$\frac{1}{R(-z)}-\frac{1}{R'(-z)} \;=\; \frac{1}{R'(z)}-\frac{1}{R(z)}, \quad \text{hence} \quad K^{-}\big|_{z_w} \;=\; K\big|_{z_w}. \tag{10}$$

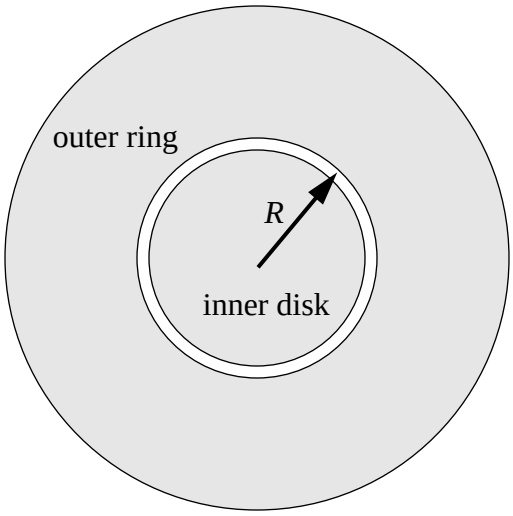

Figure 1: Circular Photodiode.

The propagators also stay unchanged, since both the sign of the direction and the sign of the *z*-axis flip. However, they have to be applied in the reverse order, i.e.

$$K^{-}_{mn,\,kl}\Big|_{z} = \sum_{op,\,qr} P_{mn,\,op} K_{op,\,qr}\Big|_{z_w} \bar{P}^{\dagger}_{qr,\,kl} \tag{11}$$

where the coordinates z and z_w together with the operators P, $\bar{P}$ and K are meant to be the same as the ones in eqn. (3).

3 CIRCULAR PHOTODETECTOR

A possible detection scheme is based on the Pound-Drever-Hall technique adapted for sensing a wavefront. In this scheme the amplitude of the 'donut' mode on the reflected light is detected by measuring the beating between a carrier 'donut' mode and the fundamental mode of the sidebands and between a sideband 'donut' mode and the fundamental mode of the carrier. Since this problem has a circular symmetry the effect is best measured with a circular photodetector (see Fig. 1).

Since we need a good common mode rejection ratio, i.e. the photodetector should be insensitive to the beating between the fundamental modes of carrier and its sidebands, the photodetector must consist of at least two segments: an inner disk and an outer ring. The signal of these two segments are subtracted from each, thus, giving maximum sensitivity for the detection of the beating between a 'donut' and a fundamental mode which has opposite signs in the inside and the outside region. The signal can be written as:

$$S_{\text{donut}} = 2\pi\left(\int_{R/w(z)}^{\infty} dr\, r - \int_{0}^{R/w(z)} dr\, r\right) U_{00} U_{\text{donut}} = \frac{4R^2}{e^{2R^2}} \tag{12}$$

where $w(z)$ is the beam spot size on the detector and R the radius which separates the inner disk from the outer ring. S_{donut} has a maximum at $R = 1/\sqrt{2}$ of $S_{\text{donut}} = 2/e$.

However, a good common mode rejection (CMR) is not necessarily achieved at the radius of largest sensitivity. Indeed, a common mode signal on a detector with a shape as described in eqn. (12) reads:

$$S_{CM} = \frac{2}{e^{2R^2}} - 1 \tag{13}$$

This common mode signal is zero at $R = \sqrt{\log\sqrt{2}} \approx 0.5887$ which is a slightly smaller radius than the one with the maximum sensitivity. But, the signal reduction is only about 6%.

4 Coupling of Optical Systems

The mode mismatch operator plays an important role, whenever two optical system are coupled together which have different eigenmode structures, or when an (input) beam with given parameters has to be coupled into an optical system which has preferred eigenmodes. Such situations occur most often between cavities, since the eigenmodes of a cavity are its resonant modes and any practical mode decomposition of the cavity field is best done in its eigenmode basis.

4.1 Input Beam Coupling

A special case of coupling two optical systems is a mode mismatch between an input beam to a cavity and the eigenmodes of this cavity. The input beam might be characterized, e.g., by the spot size and the radius of curvature at the input mirror, or alternatively by the waist size and its position on the optical axis. In both cases a mode mismatch operator can be used to transform the given input beam into a representation of the cavity eigenmodes.

$$E_{inp} = K_{inp}(w_0', z_{w_0}', w_0, z_{w_0}) \otimes E_{inp}' \tag{14}$$

where w_0 and z_{w_0} are the waist size and the waist position, respectively. The prime is used to denote the parameters of the input beam, whereas parameters without a prime are used for the (recycling) cavity modes.

4.2 Coupling of Cavities

If two cavities with different eigenmodes are coupled together, one has to define the two mode mismatch operators for the light traveling in opposite directions. For the LIGO interferometer the two arm cavities have to be coupled to the recycling cavity. If the reflected, the transmitted and the circulating field of an arm cavity with index i are written as (see section 3.1 of ref. [2])

$$E^i_{refl} = M^i_{refl} E^i_{in}, \quad E^i_{trans} = M^i_{trans} E^i_{in} \quad \text{and} \quad E^i_{circ} = M^i_{circ} E^i_{in} \tag{15}$$

the mode mismatching is introduced by

$$E^i_{refl} = K^{-}(w_0, z_{w_0}, w^i_0, z^i_{w_0}) M^i_{refl} K(w_0, z_{w_0}, w^i_0, z^i_{w_0}) E^i_{in} \equiv \overline{M}^i_{refl} E^i_{in}, \tag{16}$$

$$E^i_{trans} = M^i_{trans} K(w_0, z_{w_0}, w^i_0, z^i_{w_0}) E^i_{in} \quad \text{and} \quad E^i_{circ} = M^i_{circ} K(w_0, z_{w_0}, w^i_0, z^i_{w_0}) E^i_{in} \tag{17}$$

Eqn. (16) defines new arm cavity operators which can then be used as new 'rear mirror' operators G_1 and G_2 in the Michelson interferometer equations (see section 3.2 of ref. [2]).

4.3 LIGO Arm Cavities

The asymmetry in the LIGO interferometer — together with the fact that the arm cavities have identical properties — poses an interesting problem for mode matching. Since the two ITM mirrors are placed at a slightly different distances from the recycling mirror, there exists no mode structure in the recycling cavity which would match to both arm cavities simultaneously. The solution is then to calculate the mode structure in the recycling cavity assuming that the two ITM mirrors are place at the average recycling cavity length and by including an intrinsic (differential) mode mismatching at the interfaces between recycling and arm cavities. This mode mismatch is usually a very small effect and can be neglected for most practical purposes (for numbers see the next section).

5 Mode Parametrization in the LIGO Interferometer

If one or both of the systems which have to be coupled together are cavities, the waist size and the waist position are functions of the radii of curvature of the two mirrors forming the cavity. The radius of curvature is given by:

$$R_i(z_i) = z_i + \frac{z_0^2}{z_i} \quad \text{with the Rayleigh length} \quad z_0 = \frac{k}{2} w_0^2 \tag{18}$$

where z_i is the mirror position relative to the waist position. A deviation of one of the cavity mirrors from its ideal curvature then induces a waist size and a waist position deviation. Or conversely, a mismatch in waist size and position can be understood as an error in curvature. One can then write:

$$\begin{bmatrix} \delta g_1 \\ \delta g_2 \end{bmatrix} = J^{-1}_{arm} \begin{bmatrix} \delta w_0 / w_0 \\ \delta z_w / z_0 \end{bmatrix} \quad \text{with} \quad g_1 = 1 + \frac{z_2 - z_1}{R_1(z_1)} \quad \text{and} \quad g_2 = 1 - \frac{z_2 - z_1}{R_2(z_2)} \tag{19}$$

For a LIGO arm cavity R_1 and R_2 would be the radii of curvature of ITM and ETM, respectively, $z_2 - z_1$ would stand for the arm cavity length L and the matrix J_{arm} would be:

$$J^{-1}_{arm} = \begin{bmatrix} -1.03 & 0.89 \\ 1.28 & 0.12 \end{bmatrix} \quad \text{and} \quad J_{arm} = \begin{bmatrix} -0.09 & 0.71 \\ 1.02 & 0.82 \end{bmatrix} \tag{20}$$

In the LIGO configuration the recycling mirror does not introduce a new degree of freedom for mode matching, since (by the definition used in this document) the nominal interferometer modes are the eigenmodes of the recycling cavity defined by the radius of curvature of the recycling mirror R_{RM}, the average radius of curvature of the ITMs and the average (common) length between recycling mirror and the ITMs l_C. One can therefore express (in first order) an error in the curvature of the recycling mirror as a common waist size and position error of the arm cavities, $\Delta\overline{w}_0$ and $\Delta\overline{z}_w$, respectively:

$$\begin{bmatrix} \delta\overline{w}_0/w_0 \\ \delta\overline{z}_w/z_0 \end{bmatrix} = J_{RC}\frac{L_C}{l_C}\begin{bmatrix} \sqrt{2}\,\delta g_{RM} \\ \delta\bar{g}_{ITM} \end{bmatrix} \quad \text{with} \quad g_{RM} = 1+\frac{l_C}{R_{RM}} \quad \text{and} \quad g'_{ITM} = 1-\frac{l_C}{R'_{ITM}}. \qquad (21)$$

where g'_{ITM} and R'_{ITM} are the g-factor and the radius of curvature of the ITM mirrors as seen by the recycling cavity.

For the LIGO configuration the vector J_{RC} becomes $J_{RC} = \begin{bmatrix} -109.5 & 109.1 \\ -126.6 & 127.2 \end{bmatrix}$. (22)

It is therefore possible to characterize curvature errors of the interferometer mirrors as deviations of from ideal g-factors. A g-factor error is related to an error in the radius of curvature with the following equation:

$$\delta R = \frac{R}{1-g}\delta g \qquad (23)$$

The factors $R/(1-g)$ are equal to 52.9 km and 13.7 km for ITM and ETM, respectively. For the recycling mirror the factor $l_C/L_C \times R/(1-g)$ becomes 24.3 km, and for the ITM as seen by the recycling cavity the factor is 24.5 km.

We now rewrite the individual waist sizes and positions of each arm cavity as differential and common ones:

$$W \equiv \begin{bmatrix} \Delta w_0/w_0 \\ \Delta z_w/z_0 \\ \overline{w}_0/w_0 \\ \overline{z}_w/z_0 \end{bmatrix} = \frac{1}{\sqrt{2}}\begin{bmatrix} -1 & 0 & 1 & 0 \\ 0 & -1 & 0 & 1 \\ 1 & 0 & 1 & 0 \\ 0 & 1 & 0 & 1 \end{bmatrix}\begin{bmatrix} w_0^{arm1}/w_0 \\ z_w^{arm1}/z_0 \\ w_0^{arm2}/w_0 \\ z_w^{arm2}/z_0 \end{bmatrix} \qquad (24)$$

For a LIGO interferometer the waist size and the Rayleigh length of an arm cavity are given by

$$w_0 = 3.50\times10^{-2}\ \text{m} \quad \text{and} \quad z_0 = 3.64\times10^{3}\ \text{m}. \qquad (25)$$

Sometimes it is convenient to use a 6-component vector W to denote the additional degree-of-freedoms coming from the waist size and position of the input beam. In the new variables the errors in the g-factor can be written as

$$\delta W = J\,\delta g \quad \text{with} \quad \delta g = \frac{1}{\sqrt{2}}\begin{bmatrix} \delta g_{ETM2} - \delta g_{ETM1} \\ \delta g_{ITM2} - \delta g_{ITM1} \\ \delta g_{ETM2} + \delta g_{ETM1} \\ 2\,L_C/l_C\,\delta g_{RM} \end{bmatrix} \quad \text{and} \quad J = \begin{bmatrix} 0.71 & -0.09 & 0 & 0 \\ 0.82 & 1.02 & 0 & 0 \\ 0 & 0 & 0.71 & -110 \\ 0 & 0 & 0.82 & -127 \end{bmatrix} \tag{26}$$

The matrix J is singular, indicating that there are only three independent degree-of-freedoms. The only allowed ratio of common waist size over common waist position mismatch which can be achieved by deviations of the mirror curvatures is 0.867. Generally, it is about a factor of 150 more critical to match the curvature of the recycling mirror to the common curvature of the ITMs than it is to match the common curvatures of ITMs and ETMs.

6 Mode Mismatch Sensitivities

The signal of a wavefront sensor dedicated to measure mode mismatching reads:

$$MMS(t, \eta, \Theta) = 2J_0(\Gamma)J_1(\Gamma)Pf_{\text{split}}\,k_{PD}^{\text{donut}}\sum_i M_i\,\delta W_i \cos(2\eta - \eta_{0i})\cos(\omega_m t + \phi_{0i}) \tag{27}$$

where P is the input laser power, J_0 and J_1 are the Bessel functions which describe the amplitude of the carrier and its sidebands for a given modulation depth Γ, f_{split} is the amount of power which is split off for the mode mismatch sensor, k_{PD}^{donut} is a factor which describes the exact shape of the photodetector and is unity for the detector described in section 3, M_i are the signal amplitudes, η is the Guoy phase of the fundamental mode between the extraction port and the photodetector, η_{0i} are the intrinsic signal Guoy phase shifts, ω_m is the modulation frequency and ϕ_{0i} are the intrinsic signal rf phase shifts. From eqn. (27) one can easily obtain the photocurrent induced in the detector by multiplying with the photodiode efficiency. Also notice, that the Guoy phase dependence includes a factor of 2, because we are looking at a beating between fundamental and second order modes.

Table 1 list the mode mismatch signals at the dark port, in reflection, at the recycling cavity pick-off, in reflection of the on-line arm cavity and in reflection for the non-resonant sideband. The variables δW_i are either the deviations from the ideal waist size or the deviations from the ideal waist position. A positive value indicates a larger waist size and a waist position which is further away from the input mirror.

The mode mismatch between the recycling cavity and the two arm cavities is a property of the interferometer and can't be changed without changing its configuration. On the other hand, the input beam might be injected into the interferometer through a system of lenses which can be adjusted to optimize the power coupling into the interferometer. Detectors for such a control system are best placed in reflection using the non-resonant sidebands.

Table 1: Mode mismatch sensor signals. Top entry in each cell is M_i (with significant values in boldface), lower-left is rf-phase, and lower-right is the guoy phase η_{0i}. The M_i are in units of w_0 for the waist size mismatch and in units of z_0 for the waist position mismatch. The units of the rf- and the guoy phases are degrees.

	mode mismatch degree-of-freedom					
	input beam		differential arm		common arm	
Port	w_0	z_w	Δw_0	Δz_w	$\overline{w_0}$	$\overline{z_w}$
Dark	$< 10^{-4}$	$< 10^{-4}$	**–10.1**	**–2.91**	$< 10^{-3}$	$< 10^{-3}$
	Q 60	Q 150	Q 90	Q 90	Q 134	Q 132
Reflected	0.21	–0.12	0.89	–0.73	**–4.90**	**4.15**
	I 39	I 129	Q 45	Q 45	I 43	I 45
Recycling cavity / 1000	3.8×10^{-2}	-2.1×10^{-2}	0.12	–0.10	–0.67	0.57
	I 15	I 105	I 45	Q 45	I 43	I 45
On-line arm reflection / 1000	1.9×10^{-2}	-1.1×10^{-2}	$\sim 3 \times 10^{-2}$	$\sim 2 \times 10^{-2}$	–0.34	0.29
	Q+5 15	Q+5 105	n.a.	n.a.	Q+5 43	Q+5 45
Reflected (non-resonant sideband)	**1.88**	**1.05**	$< 10^{-3}$	$< 10^{-3}$	**–1.03**	**–0.30**
	I 150	I 60	n.a.	n.a.	I 90	I 90

In the LIGO interferometer there is a small intrinsic mode mismatch due to the asymmetry. This effect produces a signal in Q-phase at the dark port of the order of 2.3×10^{-4} in the units of Table 1 with a guoy phase shift of 90 degree. The signals at the other ports are even smaller and completely negligible.

7 GW-Signal due to Mode Mismatch

Since a mode mismatch introduces a phase shift to the fundamental mode in first order (see eqn. (8)), the gravitational wave signal at the dark port shows a first order dependence on the mode matching.

$$GWS_{MM}(\overrightarrow{\delta W}) = \overrightarrow{N}\overrightarrow{\delta W} + \frac{1}{2}\overrightarrow{\delta W} H_{sng}^{MM} \overrightarrow{\delta W} \tag{28}$$

Considering only mode mismatching of the input beam, the coefficients of N and H_{sng}^{MM} are of order 10^{-14} m (per mismatch in relative units) or lower. If we require that the gravitational wave signal at 150 Hz due to jitter in the mode matching is smaller than 5×10^{-21} m$/\sqrt{\text{Hz}}$, then the mode matching jitter at 150 Hz has to be smaller than $5 \times 10^{-7}/\sqrt{\text{Hz}}$ for the waist size/position mismatch in relative units.

8 GW-Sensitivity Loss due to Mode Mismatch

8.1 Signal Sensitivity

To obtain the loss of gravitational wave detection sensitivity we closely follow the derivation for the loss of sensitivity due to angular misalignment in ref. [4] and write the signal sensitivity as:

$$S_{sens}(\overrightarrow{\delta W}) = S_{sens}(0)\left[1 + \frac{1}{2}\overrightarrow{\delta W} H^{MM}_{sens} \overrightarrow{\delta W}\right] \tag{29}$$

The eigenvalues of the matrix H^{MM}_{sens} considering only the mode matching of the input beam are listed in Table 2. In order to prevent a degradation of the gravitational-wave detection sensitivity of more than 0.5%, the waist size of the input beam has to be adjusted within a precision of 7% of the arm cavity waist size and the waist position has to be adjusted within 12% of the arm cavity Rayleigh length.

8.2 Light Intensities

One possible way to match the input beam to the interferometer — apart from using a wavefront sensor — is to maximize the power level in the recycling or the arm cavities, or alternatively, to minimize the power in reflection. As one would expect the power levels in the interferometer depend on the mode matching in second order only and can be written as:

$$P(\overrightarrow{\delta W}) = P(0)\left[1 + \frac{1}{2}\overrightarrow{\delta W} H^{MM}_{power} \overrightarrow{\delta W}\right] \tag{30}$$

Table 2 lists the eigenvalues of the matrix H^{MM}_{power} at the dark port, in reflection, inside the recycling cavity and inside one of the arm cavities. For these calculations only the mode matching of the input beam was considered. Not surprisingly, it can be seen from Table 2 that the gravitational-wave detection sensitivity closely follows the power level in the arm cavities.

Table 2: Gravitational-wave sensitivity and power loss due to mode mismatch. The matrices H^{MM}_{sens} and H^{MM}_{power} and, therefore, also $H^{MM}_{s/n}$ are diagonal in the basis of the waist size and position. Hence, only the eigenvalues are listed. They are in units of w_0^2 for the waist size mismatch and in units of z_0^2 for the waist position mismatch, respectively.

input beam	s/n.	sens.	power levels			
	dark	dark	dark	reflect.	recycle.	arms
Δw_0	–1.88	–2.50	–1.23	49.7	–2.36	–2.50
Δz_w	–0.59	–0.78	–0.38	15.5	–0.74	–0.78

As it turns out the power level of the reflected beam is most sensitive to the mode matching of the input beam. Minimizing the power in reflection with a precision of 10% is sufficient to prevent a

loss of gravitational-wave detection sensitivity of more than 0.5%. On the other hand, the power optimization in one of the arm cavities has to be done with a precision of 0.5%.

8.3 SIGNAL-TO-NOISE

The signal to noise at the dark port for gravitational-wave detection can be written as:

$$\frac{S_{sens}(\overrightarrow{\delta W})}{\sqrt{NP(\overrightarrow{\delta W})}} = \frac{S_{sens}(0)}{\sqrt{NP(0)}}\left[1 + \frac{1}{2}\overrightarrow{\delta W} H_{s/n}^{MM} \overrightarrow{\delta W}\right] \tag{31}$$

Table 3 lists the eigenvalues and eigenvectors of the Hessian matrix $H_{s/n}^{MM}$. Since the shot noise is non-stationary, the function NP is the sum of the carrier power and 3/2 times the sideband power.

Table 3: Gravitational-wave signal-to-noise loss at the dark port due to mode mismatch. Both eigenvalues and eigenvectors of the Hessian matrix $H_{s/n}^{MM}$ are listed. The eigenvalues are in dimensionless units, whereas the eigenvectors are given in relative units. It is worthwhile to note that for all directions except m_1 the signal loss dominates over the increase of noise, where for m_1 the increase of power at the dark port is the most important effect.

eigenvector	eigenvalue	mode mismatch degree-of-freedom					
		input beam		differential arm		common arm	
		$\delta w_0/w_0$	$\delta z_w/z_0$	$\delta w_0/w_0$	$\delta z_w/z_0$	$\delta w_0/w_0$	$\delta z_w/z_0$
m_1	–354	0	0	**0.967**	0.256	–0.001	0.001
m_2	–350	0.038	–0.011	–0.001	0	**–0.759**	**0.650**
m_3	–10.2	0	0	–0.256	**0.967**	0	0
m_4	–1.63	**0.864**	**0.283**	0	0	**–0.247**	**–0.334**
m_5	–0.721	**0.466**	**–0.757**	0	0	**0.317**	**0.330**
m_6	–0.0032	0.185	**0.589**	0	0	**0.512**	**0.598**

Since a common curvature mismatch dominantly produces a common signal $\hat{m}$ with a ratio of waist size to waist position error of 0.867, it is interesting to see which linear combination of eigenvectors would lead in such a direction

$$\hat{m} = -0.006m_2 - 0.414m_4 + 0.457m_5 + 0.787m_6 \quad \text{and} \quad \hat{m} H_{s/n}^{MM} \hat{m} = -0.445\,. \tag{32}$$

The eigenvector m_2 and, hence, its eigenvalue makes only a small contribution. Or, in other words, m_2 is almost orthogonal to the dominant common mode mismatch ‘direction’ and, therefore, its large eigenvalue has no importance.

8.4 Radius of Curvature

One can now derive requirements for the radii of curvatures of the interferometer mirrors based on the degradation of the signal-to-noise at the dark port. One important thing to notice is that a curvature error of the recycling mirror or a common curvature error of the ITMs or ETMS can be partly corrected for by reoptimizing the input beam parameters. For these cases the loss of sensitivity can be minimized by replacing

$$\hat{m} \rightarrow \tilde{m} \equiv \hat{m} + \left[0.273\ 0.708\ 0\ 0\ 0\ 0\right]^T \quad \text{and} \quad \tilde{m} H_{\mathrm{s/n}}^{MM} \tilde{m} = -0.0118 \tag{33}$$

Since a readjustment of the input beam is a common change, it does have negligible influence on differential curvature errors. Using eqns. (23), (26), (31) and (33), taking the values from Table 3 and demanding that the signal-to-noise ratio at the dark port must not be degraded more than 0.5%, one can derive requirements for the mirror radii of curvature (see Table 4). The table lists maximum values for both the recycling mirror curvature error and the common ITM curvature error. Theses requirements do not have to be meet simultaneously, only the differential curvature error is of importance, whereas a common curvature error in both recycling mirror and the two ITMs is much less sensitive to mode matching.

Table 4: Requirements on the radii of curvature due to loss of signal-to-noise. Requirements are derived from the decrease in signal-to-noise ratio of the gravitational-wave read-out at the dark port. A maximum loss of 0.5% yields each of the curvature errors below. The values are given in meters.

$\lvert R_{ITM2}\text{-}R_{ITM1}\rvert$	$\lvert R_{ETM2}\text{-}R_{ETM1}\rvert$	δR_{ETM}	δR_{ITM}	δR_{RM}
~800	115	>1000	140	95

The values of Table 4 are obtained by a second order approximation around the perfectly mode matched interferometer. However, for the recycling mirror this approximation does not hold for the range indicated. Fig. 2 plots the loss of signal-to-noise for the gravitational wave readout at the dark port as a function of the radius of curvature error of the recycling mirror. For each point the input beam was reoptimized along the direction indicated in eqn. (33) to give the maximum signal-to-noise ratio at the dark port. It can be seen that for positive error values the signal-to-noise loss grows faster than expected, whereas for negative error values it grows slower than expected. Also note that for error values above +40 m the recycling cavity becomes an unstable resonator.

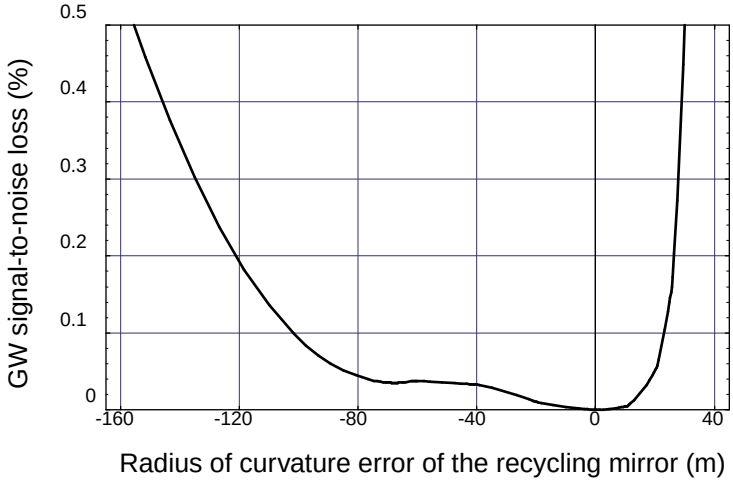

Figure 2: Gravity wave signal-to-noise loss as a function of the recycling mirror radius of curvature. The recycling cavity becomes an unstable resonator, if the curvature is changed by more than +40 m. At each point of the function the input beam parameters were reoptimized to obtain maximum sensitivity.

REFERENCE

[1] Y. Hefetz, N. Mavalvala and D. Sigg, *"Principles of calculating alignment signals in complex optical interferometers"*, LIGO-P960024-00-D (1996).

[2] D. Sigg, *"Modal model update 1: Interferometer operators"*, LIGO-T960113-00-D (1996).

[3] D. Sigg, *"Wavefront sensor"*, LIGO-T960111-00-D (1996).

[4] D. Sigg, *"Modal model update 2: GW-sensitivity to angular misalignments"*, LIGO-T960114-00-D (1996).

[5] D. Sigg, *"Modal model update 3: Small angle regime"*, LIGO-T960115-00-D (1996).